Lagrangian decomposition of the Hadley and Ferrel cells

J. Kjellsson[1] and K. Döös[1]

Received 22 May 2012; revised 5 July 2012; accepted 6 July 2012; published 11 August 2012.

[1] The meridional overturning circulation of the atmosphere between 45°S and 45°N is decomposed using simulated 3D Lagrangian trajectories for calculating the Lagrangian overturning streamfunctions. This permits an analysis of meridional mass transports which otherwise cancel in time-averaged zonal-mean Eulerian streamfunctions. Overturning circulations inferred from trajectories of no net meridional transport are qualitatively similar to the Eulerian mean, but yield half the Hadley cell amplitude, and twice that of the Ferrel cell. Cross-equatorial transports of some 130 Sv result in two cells that account for the remainder of the Hadley cells. The overturning in midlatiudes is partly cancelled by large (>150 Sv) meridional transports approximately following isentropes. Changes and implications for various coordinate systems, e.g., isentropic, are also discussed. **Citation:** Kjellsson, J., and K. Döös (2012), Lagrangian decomposition of the Hadley and Ferrel cells, *Geophys. Res. Lett.*, *39*, L15807, doi:10.1029/2012GL052420.

1. Introduction

[2] The meridional overturning circulation of the atmosphere describes the mass transport between the tropics and poles at different altitudes, which is perhaps the most fundamental property of the general circulation. Understanding this mass transport is thus important for understanding the transport of energy and atmospheric constituents (e.g., carbon dioxide), as well as their response to a changing climate. However, as the circulation is three-dimensional and time-dependent, it can be rather difficult to represent accurately in one picture. Conventional Eulerian meridional overturning streamfunctions, which represent the time-averaged zonal-mean mass transport above a certain pressure level at a certain latitude, show a three-cell structure in each hemisphere; the Hadley, Ferrel, and Polar cells [cf. *Kållberg et al.*, 2005]. However, the results differ whether the zonal mean is taken on isobars or isentropes [*Townsend and Johnson*, 1985; *Pauluis et al.*, 2010; *Döös and Nilsson*, 2011], where the latter yields only one cell in each hemisphere. Furthermore, the circulation on moist isentropes has been found stronger than that on dry isentropes [*Pauluis et al.*, 2010; *Laliberté et al.*, 2012]. Calculating the Transformed Eulerian Mean (TEM) [*Andrews and McIntyre*, 1976; *Karoly et al.*, 1997; *Held and Schneider*, 1999; *Juckes*, 2001], and recently the Statistical TEM [*Pauluis et al.*, 2011], thus including an eddy-induced contribution, yields two hemisphere-wide cells, as the Eulerian mean and eddy-induced circulations partly cancel each other in midlatitudes. It was also shown by *McIntosh and McDougall* [1996], that the TEM formulation is a approximation of the isentropic circulation in isobaric coordinates.

[3] In the present study, the meridional overturning circulation of the atmosphere is investigated using mass transports from model-simulated Lagrangian trajectories and the corresponding Lagrangian streamfunctions [*Blanke et al.*, 1999; *Döös et al.*, 2008], rather than using Eulerian methods. The Hadley and Ferrel cells are decomposed by separating the trajectories into classes depending at which latitudes they start and end. The Lagrangian streamfunction is calculated separately for each class. Thus, the overturning circulation is decomposed into parts of net meridional transport, and other parts of no net meridional transport. Information about the mean vertical displacement of trajectories in the different components of the overturning will be presented and discussed. The question of how well the conventional Eulerian mean can describe paths of Lagrangian particles will also be dealt with. In calculating the overturning circulation from intrinsic transports, it is possible to quantify and visualize some of the cancellations in it, and thus understand the paths of meridional mass transports.

2. Lagrangian Trajectories

[4] Lagrangian trajectories were calculated using the TRACMASS Lagrangian trajectory code [*Döös*, 1995; *Blanke and Raynaud*, 1997] with surface pressure and horizontal winds on model levels from the ERA-Interim data set [*Berrisford et al.*, 2009], with 6-hourly output. TRACMASS uses the 3D field of mass fluxes to compute the trajectory of a mass element [*de Vries and Döös*, 2001]. Trajectories are calculated using only mass continuity, with no parameterization such as convection or small-scale turbulence. This is in contrast to many other trajectory schemes (based on, e.g., Runge-Kutta integrations) where position is calculated from the velocity fields. A TRACMASS trajectory traveling from grid box A to B can be considered as the mass in A being transported to B. Thus, each time a trajectory crosses a grid box wall in any direction, it can be registered as a mass transport through that wall. Note that trajectories do not represent individual particles or small air parcels, but rather entire grid boxes being advected. Integrating the mass transports temporally, zonally, and vertically yields the Lagrangian streamfunction in model coordinates [*Blanke et al.*, 1999; *Döös et al.*, 2008], which may then be interpolated to pressure levels. How well trajectories represent the global-scale overturning may be found by comparing the Lagrangian and Eulerian streamfunctions.

[5] The ERA-Interim data used in this study had a horizontal resolution of 1.25° with 60 hybrid-coordinate levels [*Simmons and Burridge*, 1981]. Horizontal winds were

[1]Department of Meteorology, Bert Bolin Centre for Climate Research, Stockholm University, Stockholm, Sweden.

Corresponding author: J. Kjellsson, Department of Meteorology, Bert Bolin Centre for Climate Research, Stockholm University, Svante Arrhenius väg 16C, SE-106 91 Stockholm, Sweden. (joakim@misu.su.se)

0094-8276/12/2012GL052420

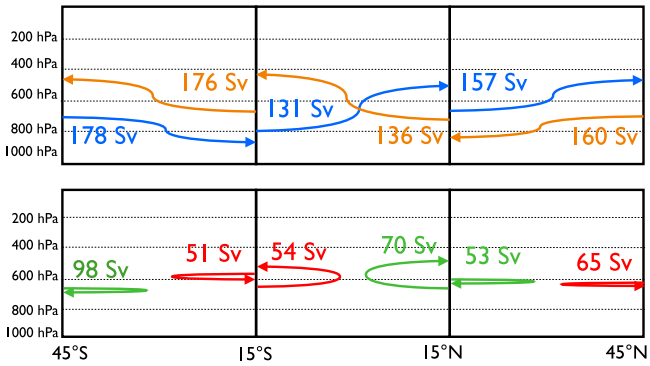

Figure 1. Schematic view of the mean pathway of each trajectory class. The green, red, yellow, and blue lines represent the classes "South to South", "North to North", "North to South", and "South to North", respectively. Maximum transport from the Lagrangian stream function is presented for each class. Units in Sv (10^9 kg/s). Mean vertical displacement for each trajectory class is roughly to scale, while the meridional displacement is only schematic.

available at each model level, and the vertical mass flux was calculated using the continuity equation (see Appendix A for discretization).

3. Meridional Overturning Streamfunctions

[6] The time-averaged zonal-mean Eulerian streamfunction in isobaric coordinates is defined as

$$\psi^E(y,p) = \frac{1}{t_1 - t_0}\int_{t_0}^{t_1}\oint_x\int_0^p \frac{v(x,y,p',t)}{g}\,dp'dxdt, \qquad (1)$$

where x, y, p' are the coordinates and $v(x, y, p', t)$ is the meridional velocity. $\psi^E(y, p)$ is then a measure of the total meridional mass flux across the latitude line y above the pressure level p averaged over the time period between t_0 and t_1. The unit of ψ^E is kg/s, however, the unit Sverdrup defined as 1 Sv = 10^9 kg/s is more practical.

[7] Let $T^y_n = (\Delta x_0 \Delta p_0 v_0)/g$ be the meridional mass transport by trajectory n. The subscript 0 denotes that T^y_n is given by its initial velocity and area, and thus remains unchanged during transit. The Lagrangian streamfunction is then, following *Blanke et al.* [1999] and *Döös et al.* [2008],

$$\psi^L_{j,k} = \sum_{k'=0}^{k}\sum_i\sum_n T^y_{i,j,k',n}, \qquad (2)$$

where $T^y_{i,j,k',n}$ is the meridional mass transport by trajectory n through the zonal-vertical grid box wall at i, j, k'. The sum over n (trajectories), i (zonal points), and to a level k at a given latitude line j is thus the total Lagrangian mass transport above level k at line j for trajectories released at a certain time. In essence, the Eulerian streamfunction uses the mass fluxes from all grid boxes within a domain, while the Lagrangian only uses those passed through by trajectories. For a high-enough number of trajectories, they should thus be very similar. The Lagrangian streamfunction differs by being derived from trajectories, which may be separated by some criteria. In this study, the criteria were such that trajectories of net meridional transport were isolated from those with no net meridional transport, and also poleward flow from equatorward flow. Hence, it is not a method to isolate eddy-induced transport as done by *Döös and Nilsson* [2011], as it is included in the trajectory motion. However, while two trajectory mass transports may cancel each other, the two separate streamfunctions show the individual transports and their magnitudes. The Lagrangian streamfunction also differs from the Lagrangian mean [*Kida*, 1977; *Bowman and Carrie*, 2002], which uses mean displacements and spread of trajectories, not mass transports.

4. Lagrangian Decomposition

[8] The meridional overturning circulation between two latitudes was decomposed by representing the circulation by Lagrangian trajectories. Model-simulated trajectories were released from all levels and longitudes at the two latitudes, every 6 hours during one year. This resulted in ~25 million trajectories for one year. Increasing this number by a factor of two did not change the results, thus ensuring that the number of trajectories was sufficiently large to sample and represent the circulation accurately. Trajectories were terminated when they reached either of the latitudes, and sorted into classes depending on their initial and final latitude. This yielded four classes for each latitude band; "North to South" ("N to S"), "South to North" ("S to N"), "North to North" ("N to N"), and "South to South" ("S to S"), the two former denoted as "inter-cell" and the two latter as "re-circulating". The Lagrangian streamfunction was then calculated for each of the four classes.

[9] This was carried out over three adjacent latitude bands, 45°S-15°S, 15°S-15°N, and 15°N-45°N. These latitude bands were roughly as wide as the overturning cells, but cut in halves such that the time-averaged zonal-mean mass flux at each boundary had a preferred direction. For example, at 15°N the Eulerian mean gives the mass flux as southward near the surface, and northward higher up, i.e., trajectories released near the surface can be expected to move southwards, ascend and then move either northwards or southwards. However, as the Hadley and Ferrel cells are far from stationary or zonally symmetric, trajectories may not adhere to the Eulerian streamlines at all. Trajectories were released in 1989, and traced until December 1991, or until they reached one of the latitudinal boundaries.

[10] Figure 1 shows a schematic view of the mean paths of each trajectory class, and the amplitudes of the corresponding Lagrangian streamfunctions (Figure 2). In calculating the mean vertical displacement, trajectories starting or ending at a pressure lower than 100 hPa (a rough estimate of the tropopause) were excluded, as they most likely are not part of the tropospheric overturning. It is noteworthy that the results were similar if this limit was instead set to 200 hPa.

[11] Figure 2 shows the Lagrangian streamfunctions for all four classes in all three latitude bands, the sum of the inter-cell Lagrangian streamfunctions, and also the sum of all Lagrangian streamfunctions. As trajectories were released every time step (6 hrs), the Lagrangian streamfunctions must be divided by the number of time steps in one year (365 × 4 = 1460) in order to be comparable to the time-averaged Eulerian mean. The total Lagrangian streamfunctions show two clear Hadley cells, each of ~30° width, stretching up to ~100 hPa, and two midlatitude Ferrel cells of smaller amplitude. Differences between the total Lagrangian and

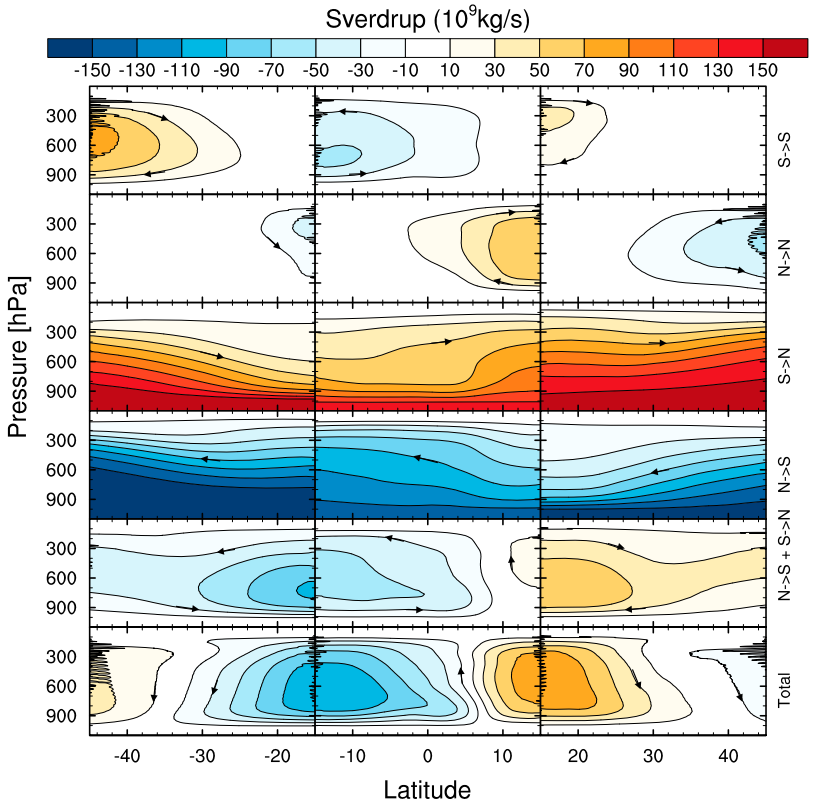

Figure 2. The Lagrangian stream functions, interpolated to isobaric coordinates, for trajectories released at 45°S, 15°S, 15°N, and 45°N every six hours during the year 1989. Units in Sv. Note that each column represents a separate simulation. Positive (red) amplitude implies clockwise circulation. The upper four rows show the Lagrangian stream function of transport between the different latitudes, where "S - S" means from the southern boundary and back to the southern boundary and so on. The fifth row shows the sum of the "N - S" and "S - N" stream functions. The total Lagrangian stream function for each latitude band is presented in the bottom row. The noise at the latitudinal boundaries are artifacts of the trajectories being traced on model levels and plotted on pressure levels.

Eulerian streamfunctions are around 10% at most, indicating that trajectories represent the paths of the meridional overturning well in a zonal mean. Similar results, but for the ocean, were noted by *Döös et al.* [2008]. In the present decomposition, the re-circulating streamfunctions resemble the Eulerian streamfunction, but of different magnitudes. Inter-cell streamfunctions, on the other hand, have larger amplitudes and shapes different from the Eulerian mean. As the poleward and equatorward inter-cell streamfunctions represent mass transports between two latitudes and sometimes at the same pressure levels, it is clear that they tend to partly cancel each other in the total result.

[12] As tropical trajectories generally ascended and exited the domain at high altitudes (Figure 1), adding the two tropical inter-cell streamfunctions yielded a net overturning of the same sign as the re-circulating streamfunctions (Figure 2). This implies that trajectories, on average, followed paths similar to Eulerian mean streamlines. In the subtropics, the situation was reversed. The re-circulating streamfunctions were found twice as strong as the total Lagrangian, while the streamlines in both the "N to S" and "S to N" classes tilted in the same direction (Figure 1) resulting in a net overturning of opposite sign (Figure 2). Thus, the Ferrel cell can be considered the residual of two opposite transports, and trajectories do not, generally, agree with Eulerian streamlines. Note that the total inter-cell streamfunctions showed similarities to the Eulerian mean averaged on isentropes [*Townsend and Johnson*, 1985; *Karoly et al.*, 1997; *Held and Schneider*, 1999], but of a smaller amplitude. It is difficult to assess the extent to which trajectories followed isentropes, but the paths tilted in the same manner [*Juckes*, 2001; *Kållberg et al.*, 2005]. Note, however, that as air is transported any longer distance, it is expected to cool diabatically from radiation.

[13] The total mass transport of each class, excluding trajectories above 100 hPa, is presented in Table 1. In all three latitude bands, the re-circulating trajectories comprised significantly larger total transports than the inter-cell classes. However, as the re-circulating trajectories by definition yield no net meridional transport, they can only contribute to the Lagrangian streamfunction if they result in net vertical displacement. On average, re-circulating trajectories in the tropics were displaced vertically by <200 hPa (Figure 1), and much less outside the tropics, where convection is not as deep. Thus the contribution of each re-circulating trajectory to the isobaric overturning streamfunction was comparatively small. The total transport of inter-cell trajectories was, by definition, equal to the magnitude of the corresponding Lagrangian streamfunction at the surface. These trajectories contribute to the total streamfunction as long as the equatorward and poleward flow occur at different isobars, which was not always the case. Differences seen between the values

Table 1. Total Mass Transport (in Sv) of Trajectories With Initial and Final Point Below 100 hPa in Each Class[a]

	45°S-15°S	15°S-15°N	15°N-45°N
N to N	473 Sv	496 Sv	900 Sv
N to S	161 Sv	129 Sv	152 Sv
S to N	171 Sv	126 Sv	140 Sv
S to S	1064 Sv	506 Sv	481 Sv

[a]Note the differences from Figure 1.

in Table 1 and Figure 1 for these classes are due to the Lagrangian streamfunctions including all trajectories, while the mass transports presented in Table 1 were based on trajectories starting and ending below the 100 hPa level. The transport to/from/within the levels above thus amount to ∼10% of the total values, indicating that most of the mass transport in the atmosphere occurs in the troposphere.

5. Discussion and Conclusions

[14] The meridional overturning circulation between the tropics and the midlatitudes in 1989 has been decomposed using Lagrangian streamfunctions, as opposed to the Eulerian time-averaged zonal-mean. It is a conclusion of this study that the total Lagrangian mass transport comprises two strong meridional flows in opposite directions, and two re-circulating flows of no net meridional displacement. This study has quantified these flows, and shown their contributions to the total meridional overturning. The re-circulating streamfunctions were qualitatively similar to the Eulerian mean, with magnitudes of 50–70 Sv for the Hadley cells (smaller than the Eulerian mean) and 65 and 98 Sv for the Ferrel cells (larger than the Eulerian mean). Inter-cell transports were ∼130 Sv in the tropics and >150 Sv between the tropics and the midlatitudes. These trajectories yielded an overturning similar to the isentropic circulation and the TEM [*McIntosh and McDougall*, 1996; *Karoly et al.*, 1997; *Held and Schneider*, 1999], although weaker as not all of the released trajectories were included. From Figure 2 it should be noted that the inter-cell streamfunction was found considerably larger for the southern Hadley cell then for the northern. This may partly be due to the large cross-equatorial mass transports associated with the Indian monsoon. The trajectory simulations were carried out for other years than 1989, yielding very similar results.

[15] The Hadley Circulations were shown to contain large cross-equatorial (inter-hemispheric) mass transports that partly cancelled. On the basis of the numbers given in Figure 1 the residual was found to be 131 − 136 = −5 Sv, which thus was the inter-hemispheric mass transport in 1989. The Eulerian mean equivalent is $\psi^E(0^\circ, p_s)$, i.e., the Eulerian streamfunction at the surface equator, which was −6 Sv. It must be noted that the Eulerian value is simply the time-averaged zonal-mean mass flux at 0° which does not necessarily represent the mass flux between 15°N and 15°S. That the time-averaged inter-hemispheric mass transport is southward was also noted by *Berrisford et al.* [2011], who suggested that this to some extent is due to errors in the reanalysis data.

[16] The amplitude and sign of the re-circulating streamfunctions may vary with the choice of vertical coordinate, but the inter-cell streamfunctions will not. However, their relative importance may well change in dry/moist isentropic coordinates. As the total Lagrangian stream function in isobaric coordinates represents the Eulerian mean well, it should do the same in isentropic coordinates. From Figure 1, the magnitude of inter-cell transports are similar to the amplitudes of the circulation on moist isentropes [*Döös and Nilsson*, 2011]. It is thus conceivable that the poleward and equatorward branches are more clearly separated in such coordinates, hence the inter-cell streamfunctions yield less cancellations, and the re-circulating streamfunctions may also be less important, such that the inter-cell streamfunctions in moist isentropic coordinates may explain most of the overturning.

[17] With the ability to decompose streamfunctions, once established, future work could be to further investigate the Lagrangian mass transport on dry and moist isentropes, in particular cancellations on dry isentropes [*Laliberté et al.*, 2012]. Also, *Laliberté and Pauluis* [2010] found that, in the 21st century, the circulation on dry isentropes may weaken while it may intensify on moist isentropes in winter. It would then be very interesting to produce Figure 2 using a climate model with future scenarios. The inter-hemispheric transport could also be examined more closely, e.g., finding the mixing pathways of the hemispheres.

Appendix A: Lagrangian Trajectories in the Atmosphere

[18] The TRACMASS trajectory code calculates Lagrangian trajectories using fields of mass flux, not velocity. In the ERA-Interim data, the vertical coordinate is a terrain-following hybrid coordinate [*Simmons and Burridge*, 1981], where the pressure at the lower interface of level k is given by $p_k = A_k + B_k p_s$, where p_s is the surface pressure and A_k and B_k are parameters at the level $k \in [0, 60]$, with $p_{60} = p_s$ and $p_0 = 0$. The meridional mass flux on model levels is obtained using the width and depth of the grid box

$$V_{i,j,k} = v_{i,j,k} \frac{\Delta x_j (\Delta A_k + \Delta B_k p_s)}{g},$$

where the relation $\Delta p_{i,j,k} = A_k - A_{k-1} + (B_k - B_{k-1}) p_s = \Delta A_k + \Delta B_k p_s$ has been used. The width Δx_j depends on the latitude while the depth varies in both space and time as p_s varies. Similar calculations can be made for the zonal mass flux, $U_{i,j,k}$. Vertical velocity is obtained from the continuity equation [*Simmons and Burridge*, 1981]:

$$\left(\dot{\eta}\frac{\partial p}{\partial \eta}\right)_k = -\frac{\partial p_k}{\partial t} - \sum_{r=1}^{k} \nabla\cdot(u_r, v_r)\Delta p_r. \tag{A1}$$

Noting that $\partial p_k/\partial t = \partial/\partial t(B_k p_s)$, and multiplying by $\Delta x \Delta y$ yields, in discretized form

$$\begin{aligned} W_k &= \Delta x \Delta y \left(\dot{\eta}\frac{\partial p}{\partial \eta}\right)_k \\ &= -\sum_{r=1}^{k} \Big(U_{i,j,r} - U_{i-1,j,r} + V_{i,j,r} - V_{i,j-1,r} \\ &\quad + \Delta x \Delta y \Delta B_r \frac{p_s^n - p_s^{n-1}}{\Delta t} \Big), \end{aligned} \tag{A2}$$

where Δt = 6 hours is the time between two consecutive fields of data at $n - 1$ and n. Thus, vertical motion is both

due to mass flux divergence, and to temporal changes in the pressure of the level interfaces. As continuity (equation (A1)) was used to obtain equation (A2), the scheme ought to conserve mass. However, due to the fact that the analysis fields from ERA-Interim are not mass-conserving in the sense that the horizontal mass fluxes of a column do not always match changes in surface pressure [*Berrisford et al.*, 2011], the vertical mass flux at the Earth's surface, $W_{k=60}$, may be non-zero. It may also be non-zero due to water vapor fluxes. To avoid trajectories penetrating the Earth's surface, the mass flux must be explicitly prescribed as zero. In effect, a trajectory may thus go infinitesimally close to the surface but not exactly at it, while being free to move horizontally.

[19] **Acknowledgments.** The authors wish to thank the two anonymous reviewers who greatly helped improve the paper, as well as Rodrigo Caballero, Peter Lundberg, and Jonas Nycander for fruitful discussions and insights. Thanks is also extended to ECMWF for processing and supplying data from the ERA-Interim data set. All trajectory computations have been carried out on the Vagn-Ekman supercomputers maintained by NSC at Linköping University, and PDC at the Royal Institute of Technology, Stockholm, Sweden. This study is a contribution from the Bert Bolin Centre for Climate Research at Stockholm University.

[20] The Editor thanks the two anonymous reviewers for assisting in the evaluation of this paper.

References

Andrews, D., and M. McIntyre (1976), Planetary waves in horizontal and vertical shear: The generalized Eliassen-Palm relation and the mean zonal acceleration, *J. Atmos. Sci.*, *33*(11), 2031–2048.

Berrisford, P., D. Dee, K. Fielding, M. Fuentes, P. Kållberg, S. Kobayashi, and S. Uppala (2009), The ERA-Interim archive, *ERA Rep. Ser.*, *1*(1), 1–16.

Berrisford, P., P. Kållberg, S. Kobayashi, D. Dee, S. Uppala, A. J. Simmons, P. Poli, and H. Sato (2011), Atmospheric conservation properties in ERA-Interim, *Q. J. R. Meteorol. Soc.*, *137*, 1381–1399.

Blanke, B., and S. Raynaud (1997), Kinematics of the Pacific Equatorial Undercurrent: An Eulerian and Lagrangian approach from GCM results, *J. Phys. Oceanogr.*, *27*, 1038–1053.

Blanke, B., M. Arhan, G. Madec, and S. Roche (1999), Warm water paths in the equatorial Atlantic as diagnosed with a general circulation model, *J. Phys. Oceanogr.*, *29*, 2753–2768.

Bowman, K. P., and G. D. Carrie (2002), The mean-meridional transport circulation of the troposphere in an idealized GCM, *J. Atmos. Sci.*, *59*, 1502–1514.

de Vries, P., and K. Döös (2001), Calculating Lagrangian trajectories using time-dependent velocity fields, *J. Atmos. Oceanic Technol.*, *18*, 1092–1101.

Döös, K. (1995), Interocean exchange of water masses, *J. Geophys. Res.*, *100*, 13,499–13,514.

Döös, K., and J. Nilsson (2011), Analysis of the meridional energy transport by atmospheric overturning circulations, *J. Atmos. Sci.*, *68*, 1806–1820.

Döös, K., J. Nycander, and A. C. Coward (2008), Lagrangian decomposition of the Deacon Cell, *J. Geophys. Res.*, *113*, C07028, doi:10.1029/2007JC004351.

Held, I. M., and T. Schneider (1999), The surface branch of the zonally averaged mass transport circulation in the troposphere, *J. Atmos. Sci.*, *56*, 1688–1697.

Juckes, M. (2001), A generalization of the transformed Eulerian-mean meridional circulation, *Q. J. R. Meteorol. Soc.*, *127*, 147–160.

Kållberg, P., P. Berrisford, B. Hoskins, A. J. Simmons, S. Uppala, S. Lamy-Thépaut, and R. Hine (2005), ERA-40 Atlas, *ERA-40 Proj. Rep. Ser.*, *19*, 191.

Karoly, D. J., P. C. McIntosh, P. Berrisford, T. J. McDougall, and A. C. Hirst (1997), Similarities of the Deacon cell in the Southern Ocean and the Ferrel cells in the atmosphere, *Q. J. R. Meteorol. Soc.*, *123*, 519–526.

Kida, H. (1977), A numerical investigation of the atmospheric general circulation and stratospheric-tropospheric mass exchange: II. Lagrangian motion of the atmosphere, *J. Meteorol. Soc. Jpn.*, *55*(1), 71–88.

Laliberté, F., and O. Pauluis (2010), Winter intensification of the moist branch of the circulation in simulations of 21st century climate, *Geophys. Res. Lett.*, *37*, L20707, doi:10.1029/2010GL045007.

Laliberté, F., T. Shaw, and O. Pauluis (2012), Moist recirculation and water vapor transport on dry isentropes, *J. Atmos. Sci.*, *69*, 875–890.

McIntosh, P. C., and T. J. McDougall (1996), Isopycnal averaging and the residual mean circulation, *J. Phys. Oceanogr.*, *26*, 1655–1660.

Pauluis, O., A. Czaja, and R. Korty (2010), The global atmospheric circulation in moist isentropic coordinates, *J. Clim.*, *23*, 3077–3093.

Pauluis, O., T. Shaw, and F. Laliberté (2011), A statistical generalization of the transformed Eulerian-Mean circulation for an arbitrary vertical coordinate system, *J. Atmos. Sci.*, *68*, 1766–1783.

Simmons, A. J., and D. M. Burridge (1981), An energy and angular-momentum conserving vertical finite-difference scheme and hybrid vertical coordinate, *Mon. Weather Rev.*, *109*, 758–766.

Townsend, R. D., and D. R. Johnson (1985), A diagnostic study of the isentropic zonally averaged mass circulation during the first GARP global experiment, *J. Atmos. Sci.*, *42*(15), 1565–1579.